FINAL REPORT: New Synthetic Methods and Structure-Property Relationships in Neptunium, Plutonium, and Americium Borates

Grant Number: DE-FG02-01ER16026

Institution: University of Notre Dame

Principal Investigator: Prof. Thomas E. Albrecht-Schmitt
Department of Civil Engineering and Geological Sciences
Department of Chemistry and Biochemistry
156 Fitzpatrick Hall
University of Notre Dame
Notre Dame, IN 46556

Grant Number: DE-FG02-01ER16026

CURRENT CONTACT INFO:
Institution: Florida State University

Principal Investigator: Prof. Thomas E. Albrecht-Schmitt
Department of Chemistry and Biochemistry
Florida State University
95 Chieftan Way
Tallahassee, Florida 32306-4390

Telephone Number: 850-645-0477
Email: talbrechtschmitt@gmail.com

DOE/Office of Science Program Office: Basic Energy Sciences, Heavy Elements Chemistry Program

DOE/Office of Science Program Technical Program Manager Contact: Dr. Philip Wilk

RESULTS FROM DOE SUPPORT

The past three years of support by the Heavy Elements Chemistry Program have been highly productive in terms of advanced degrees awarded, currently supported graduate students, peer-reviewed publications, and presentations made at universities, national laboratories, and at international conferences. Ph.D. degrees were granted to Shuao Wang and Juan Diwu, who both went on to post-doctoral appointments at the Glenn T. Seaborg Center at Lawrence Berkeley National Laboratory with Jeff Long and Ken Raymond, respectively. Pius Adelani completed his Ph.D. with me and is now a post-doc with Peter C. Burns. Andrea Alsobrook finished her Ph.D. and is now a post-doc at Savannah River with Dave Hobbs. Anna Nelson completed her Ph.D. and is now a post-doc with Rod Ewing at the University of Michigan. As can be gleaned from this list, students supported by the Heavy Elements Chemistry grant have remained interested in actinide science after leaving my program. This follows in line with previous graduates in this program such as Richard E. Sykora, who did his post-doctoral work at Oak Ridge National Laboratory with R. G. Haire, and Amanda C. Bean, who is a staff scientist at Los Alamos National Laboratory, and Philip M. Almond and Thomas C. Shehee, who are both staff scientists at Savannah River National Laboratory, Gengbang Jin who is a staff scientist at Argonne National Lab, and Travis Bray who has been a post-doc at both LBNL and ANL. Clearly this program is serving as a pipe-line for students to enter into careers in the national laboratories. About half of my students depart the DOE complex for academia or industry. My undergraduate researchers also remain active in actinide chemistry after leaving my group. Dan Wells was a productive undergraduate of mine, and went on to pursue a Ph.D. on uranium and neptunium chalcogenides with Jim Ibers at Northwestern. After earning his Ph.D., he went directly into the nuclear industry.

The following papers, specifically supported by this grant, were published from 2010 to early 2013.

54. M. J. Polinski, E. V. Alekseev, V. R. Darling, J. N. Cross, W. Depmeier, T. E. Albrecht-Schmitt, "New Family of Lanthanide Borate Halides with Unusual Coordination including a Neodymium-Containing Cationic Framework," *Inorganic Chemistry*, **2013**, *52*, 1965-1975.

53. J.-M. Babo, T. E. Albrecht-Schmitt, "High Temperature Synthesis of Two Open-Framework Uranyl Silicates with Ten-Ring Channels: $Cs_2(UO_2)_2Si_8O_{19}$ and $Rb_2(UO_2)_2Si_5O_{13}$," *Journal of Solid State Chemistry*, **2013**, *197*, 186-190.

52. S. Wu, S. Wang, M. Polinski, O. Beermann, P. Kegler, T. Malchereck, A. Holzheid, W. Depmeier, D. Bosbach, T. E. Albrecht-Schmitt, E. V. Alekseev, "High Structural Complexity of Potassium Uranyl Borates Derived from High-Temperature / High-Pressure Conditions," *Inorganic Chemistry*, **2013**, *52*, 5110-5118.

51. P. O. Adelani, T. E. Albrecht-Schmitt, "Layered Uranyl Coordination Polymers Rigidly Pillared by Diphosphonates," *Crystal Growth & Design*, **2012**, *12*, 5800-5805.

50. M. J. Polinski, S. Wang, E. V. Alekseev, J. N. Cross, W. Depmeier, T. E. Albrecht-Schmitt, "Effect of pH and Reaction Time on the Structures of Early Lanthanide(III) Borate Perchlorates," *Inorganic Chemistry*, **2012**, *51*, 11541-11548. DOI: 10.1021/ic301421e.

49. M. J. Polinski, S. Wang, J. N. Cross, E. V. Alekseev, W. Depmeier, T. E. Albrecht-Schmitt, "Effects of Large Halides on the Structures of Lanthanide(III) and Plutonium(III) Borates," *Inorganic Chemistry*, **2012**, *51,* 7859-7866. DOI:10.1021/ic3009317.

48. S. Wang, J. Diwu, E. V. Alekseev, L. J. Jouffret, W. Depmeier, T. E. Albrecht-Schmitt, "Cation-Cation Interactions Between Neptunyl(VI) Units," *Inorganic Chemistry*, **2012**, *51*, 7016-7018. DOI:10.1021/ic3009305.

47. M. J. Polinski, D. J. Grant, S. Wang, E. V. Alekseev, J. N. Cross, E. M. Villa,W. Depmeier, L. Gagliardi, T. E. Albrecht-Schmitt, "Differentiating between Trivalent Lanthanides and Actinides," *Journal of the American Chemical Society*, **2012**, *134*, 10682-10692. DOI:10.1021/ja303804r.

46. J. Diwu, S. Wang, T. E. Albrecht-Schmitt, "Periodic Trends in Lanthanide and Actinide Phosphonates: Discontinuity between Plutonium and Americium," *Inorganic Chemistry*, **2012**, *51*, 6906-6915. DOI:10.1021/ic300742p.

45. J. Diwu, T. E. Albrecht-Schmitt, "Mixed-Valent Uranium(IV,VI) Diphosphonate: Synthesis, Structure, and Spectroscopy," *Inorganic Chemistry*, **2012**, *51*, 4432-4434. DOI:10.1021/ic300391p.

44. S. Wang, T. G. Parker, J. Diwu, W. Depmeier, E. V. Alekseev, T. E. Albrecht-Schmitt, "Elucidation of the Structure of Tetraboric Acid with a New Borate Fundamental Building Block in a Chiral Uranyl Fluoroborate," *Inorganic Chemistry*, **2012**, *ASAP*.

43. S. Wu, P. Kegler, S. Wang, A. Holzheid, W. Depmeier, T. Malcherek, E. V. Alekseev, T. E. Albrecht-Schmitt, "Rich coordination of Nd^{3+} in $Mg_2Nd_{13}(BO_3)_8(SiO_4)_4(OH)_3$, derived from high-pressure/high-temperature conditions," *Inorganic Chemistry*, **2012**, *51*, 3941-3943. DOI:10.1021/ic3002493.

42. J.-M. Babo, T. E. Albrecht-Schmitt, "High Temperature Synthesis of Two Open-Framework Uranyl Silicates with Ten-Ring Channels: $Cs_2(UO_2)_2Si_8O_{19}$ and $Rb_2(UO_2)_2Si_5O_{13}$," *Journal of Solid State Chemistry*, **2013**, *197*, 186-190. DOI: 10.1016/j.jssc.2012.07.048

41. S. Wu, O. Beermann, S. Wang, A. Holzheid, W. Depmeier, T. Malcherek, G. Modolo, E. V. Alekseev, T. E. Albrecht-Schmitt, "Synthesis of Uranium Materials under Extreme Conditions: $UO_2[B_3Al_4O_{11}(OH)]$, a Complex 3D Aluminoborate," *Chemistry-A European Journal*, **2012**, *18*, 4166-4169. DOI:10.1002/chem.201200505.

40. P. O. Adelani, A. G. Oliver, T. E. Albrecht-Schmitt, "Uranyl Heteropolyoxometalate: Synthesis, Structure, and Spectroscopic Properties," *Inorganic Chemistry*, **2012**, *51*, 4885-4887. DOI:10.1021/ic300035n.

39. J. Diwu, T. E. Albrecht-Schmitt, "Chiral Uranium Phosphonates Constructed from Achiral Units with Framework Structures," *Chemical Communications*, **2012**, *48*, 3827-3829. DOI:10.1039/c2cc30519d.

38. G. K. Liu, S. Wang, T. E. Albrecht-Schmitt, M. P. Wilkerson, "Electronic Transitions and Vibronic coupling in Neptunyl Compounds," *Journal of Physical Chemistry A*, **2012**, *116,* 8297-8302. DOI:10.1021/jp302679q.

37. S. Wu, S. Wang, J. Diwu, W. Depmeier, T. Malcherek, E. V. Alekseev, T. E. Albrecht-Schmitt, "Complex Clover Cross-Sectioned Nanotubules Exist in the Structure of First Uranium Borate Phosphate," *Chemical Communications* **2012**, *48*, 3479-3481. *Featured on Cover.* DOI:10.1039/c2cc17517g.

36. M. J. Polinski, S. Wang, E. V. Alekseev, W. Depmeier, G. Liu, R. G. Haire, T. E. Albrecht-Schmitt, "Curium(III) Borate Reveals Coordination Environments of both Plutonium(III) and Americium(III) Borates," *Angewandte Chemie*, *Int. Ed.*, **2012**, *51*, 1869-1872. DOI:10.1002/anie.201107956.

35. J. Diwu, S. Wang, T. E. Albrecht-Schmitt, "Periodic Trends in Hexanuclear Actinide Clusters," *Inorganic Chemistry*, **2012**, *51*, 4088-4093. DOI:10.1021/ic2023242.

34. P. O. Adelani, T. E. Albrecht-Schmitt, "Thorium and Uranium Diphosphonates: Syntheses, Structures, and Spectroscopic Properties," *Journal of Solid State Chemistry*, **2012**, *192*, 377-384. DOI:10.1016/j.jssc.2012.04.017.

33. A.-G. D. Nelson, R. C. Ewing, T. E. Albrecht-Schmitt, "Barium Uranyl Diphosphonates," *Journal of Solid State Chemistry*, **2012**, *192,* 153-160. DOI:10.1016/j.jssc.2012.04.002.

32. S. Wang, E. V. Alekseev, W. Depmeier, T. E. Albrecht-Schmitt, "Evidence for the Presence of Neptunium(IV) within New Neptunium(V) Borates," *Inorganic Chemistry* **2012**, *51*, 7-9. DOI:10.1021/ic201682s.

31. P. O. Adelani, T. E. Albrecht-Schmitt, "Metal-Controlled Assembly of Uranyl Diphosphonates toward the Design of Functional Uranyl Nanotubules," *Inorganic Chemistry*, **2011**, *50*, 12184-12191. *Selected for Cover Art Feature.* DOI:10.1021/ic201945p.

30. P. O. Adelani, T. E. Albrecht-Schmitt, "Heterobimetallic Copper(II) Uranyl Carboxyphenylphosphonates," *Crystal Growth & Design*, **2011**, *11*, 4676-4683. DOI:10.1021/cg200978y.

29. P. O. Adelani, T. E. Albrecht-Schmitt, "Syntheses of Uranyl Diphosphonate Compounds Using Encapsulated Cations as Structure Directing Agents," *Crystal Growth & Design*, **2011**, *11*, 4227-4239. DOI:10.1021/cg200872a.

28. S. Wang, E. V. Alekseev, W. Depmeier, T. E. Albrecht-Schmitt, "Recent Progress in Actinide Borate Chemistry," *Chem. Commun.* **2011**, *47*, 10874-10885. *Invited Highlight.* DOI:10.1039/c1cc14023j.

27. M. J. Polinski, S. Wang, E. V. Alekseev, W. Depmeier, T. E. Albrecht-Schmitt, "Bonding Changes in Plutonium(III) and Americium(III) Borates," *Angewandte Chemie*, *Int. Ed.*, **2011**, *50*, 8891-8894. DOI:10.1002/anie.201103502.

26. P. O. Adelani, A. G. Oliver, T. E. Albrecht-Schmitt, "Layered and Three-Dimensional Framework Cesium and Barium Uranyl Carboxyphenylphosphonates," *Crystal Growth & Design*, **2011**, *11*, 3072-3080. DOI:10.1021/cg200337w.

25. S. Wang, E. V. Alekseev, W. Depmeier, T. E. Albrecht-Schmitt, "$K(NpO_2)_3(H_2O)Cl_4$: A Channel Structure Assembled by Two- and Three-Center Cation-Cation Interactions of Neptunyl Cations," *Inorganic Chemistry*, **2011**, *50*, 4692-4694. DOI:10.1021/ic200549f.

24. P. O. Adelani, T. E. Albrecht-Schmitt, "Pillared and Open-Framework Uranyl Diphosphonates," *Journal of Solid State Chemistry*, **2011**, *184*, 2368-2373. DOI:10.1016/j.jssc.2011.06.039.

23. S. Wang, E. V. Alekseev, J. Diwu, H. M. Miller, A. G. Oliver, G. Liu, W. Depmeier, T. E. Albrecht-Schmitt, "Syntheses, Crystal Structures, and Nonlinear Optical Properties of Novel Actinide Fluoroborates," *Chemistry of Materials*, **2011**, *23*, 2931-2939. DOI:10.1021/cm2004984.

22. P. O. Adelani, A. G. Oliver, T. E. Albrecht-Schmitt, "Hydrothermal Synthesis and Structural Characterization of Organically Templated Uranyl Diphosphonates," *Crystal Growth & Design*, **2011**, *11*, 1966-1973. DOI:10.1021/cg200129g.

21. A. N. Alsobrook, E. V. Alekseev, W. Depmeier, T. E. Albrecht-Schmitt, "Incorporation of Mn(II) and Fe(II) into Uranyl Carboxyphosphonates," *Crystal Growth & Design*, **2011**, *11*, 2358-2367. DOI:10.1021/cg200127a.

20. S. Wang, E. V. Alekseev, W. Depmeier, T. E. Albrecht-Schmitt, "Surprising Coordination for Plutonium in the First Plutonium(III) Borate," *Inorganic Chemistry*, **2011**, *50*, 2079-2081. DOI:10.1021/ic200064n.

19. J. Diwu, J. J. Good, V. H. DiStefano, T. E. Albrecht-Schmitt, "Self-Assembly of Hexanuclear Clusters of 4f and 5f Elements with Cation Specificity," *European Journal of Inorganic Chemistry*, **2011**, *2011*, 1374-1377. DOI:10.1002/ejic.201100066.

18. A. N. Alsobrook, B. G. Hauser, J. T. Hupp, E. V. Alekseev, W. Depmeier, T. E. Albrecht-Schmitt, "From Layered Structures to Cubic Frameworks: Expanding the Structural Diversity of Uranyl Carboxyphosphonates via the Incorporation of Cobalt," *Crystal Growth & Design*, **2011**, *11*, 1385-1393. DOI:10.1021/cg101668f.

17. J. Diwu, S. Wang, J. J. Good, V. H. DiStefano, T. E. Albrecht-Schmitt, "Deviation Between the Chemistry of Ce(IV) and Pu(IV) and Routes to Ordered and Disordered Heterobimetallic 4f/5f and 5f/5f Phosphonates," *Inorganic Chemistry*, **2011**, *50*, 4842-4850. DOI:10.1021/ic200006m.

16. A. N. Alsobrook, B. G. Hauser, J. T. Hupp, E. V. Alekseev, W. Depmeier, T. E. Albrecht-Schmitt, "Uranyl Carboxyphosphonates that Incorporate Cd(II)," *Journal of Solid State Chemistry*, **2011**, *184*, 1195-1200. DOI:10.1016/j.jssc.2011.03.026.

15. S. Wang, E. M. Villa, J. Diwu, E. V. Alekseev, W. Depmeier, T. E. Albrecht-Schmitt, "Role of Anions and Reaction Conditions in the Preparation of Uranium(VI), Neptunium(VI), and Plutonium(VI) Borates," *Inorganic Chemistry*, **2011**, *50*, 2527-2533. DOI:10.1021/ic102356d.

14. A. N. Alsobrook, B. G. Hauser, J. T. Hupp, E. V. Alekseev, W. Depmeier, T. E. Albrecht-Schmitt, "Cubic and Rhombohedral Heterobimetallic Networks Constructed from Uranium, Transition Metals, and Phosphonoacetate: New Methods for Constructing Porous Materials," *Chemical Communications* **2010**, *46*, 9167-9169. DOI:10.1039/c0cc03507f.

13. S. Wang, E. V. Alekseev, H. M. Miller, W. Depmeier, T. E. Albrecht-Schmitt, "Boronic Acid Flux Synthesis and Crystal Growth of Uranium and Neptunium Boronates and Borates: A Low Temperature

Route to the First Neptunium(V) Borate," *Inorganic Chemistry*, **2010**, *49*, 9755-9757. DOI:10.1021/ic101678d.

12. J. Diwu, S. Wang, Z. Liao, T. E. Albrecht-Schmitt, "Cerium(IV), Neptunium(IV), and Plutonium(IV) 1,2-phenyldiphosphonates: Correlations and Differences between Early Transuranium Elements and Their Proposed Surrogates," *Inorganic Chemistry*, **2010**, *49*, 10074-10080. DOI:10.1021/ic1015912.
11. S. Wang, E. V. Alekseev, J. T. Stritzinger, G. Liu, W. Depmeier, T. E. Albrecht-Schmitt, "Structure-Property Relationships in Lithium, Silver, and Cesium Uranyl Borates," *Chemistry of Materials*, **2010**, *22*, 5983-5991. DOI:10.1021/cm1022135.
10. P. O. Adelani, T. E. Albrecht-Schmitt, "Differential Ion Exchange in Elliptical Uranyl Diphosphonate Nanotubules," *Angewandte Chemie*, *Int. Ed.*, **2010**, 8909-8911. DOI:10.1002/anie.201004797.
9. S. Wang, E. V. Alekseev, J. T. Stritzinger, W. Depmeier, T. E. Albrecht-Schmitt, "Crystal Chemistry of the Potassium and Rubidium Uranyl Borate Families Derived from Boric Acid Fluxes," *Inorganic Chemistry*, **2010**, *49*, 6690-6696. DOI:10.1021/ic100728s.
8. P. O. Adelani, T. E. Albrecht-Schmitt, "Comparison of Thorium(IV) and Uranium(VI) Carboxyphosphonates," *Inorganic Chemistry*, **2010**, *49*, 5701-5705. DOI:10.1021/ic1006132.
7. S. Wang, E. V. Alekseev, W. Depmeier, T. E. Albrecht-Schmitt, "Further Insights into Intermediate- and Mixed-Valency in Neptunium Oxoanion Compounds: Structure and Absorption Spectroscopy of $K_2[(NpO_2)_3B_{10}O_{16}(OH)_2(NO_3)_2]$," *Chemical Communications* **2010**, 46, 3955-3957. *Invited Article.* DOI:10.1039/c002588g.
6. S. Wang, E. V. Alekseev, J. T. Stritzinger, W. Depmeier, T. E. Albrecht-Schmitt, "How are Centrosymmetric and Noncentrosymmetric Structures Achieved in Uranyl Borates?," *Inorganic Chemistry*, **2010**, *49*, 2948-2953. DOI:10.1021/ic902480n.
5. S. Wang, E. V. Alekseev, J. Ling, G. Liu, W. Depmeier, T. E. Albrecht-Schmitt, "Polarity and Chirality in Uranyl Borates: Insights into Understanding the Vitrification of Nuclear Waste and the Development of Nonlinear Optical Materials," *Chemistry of Materials*, **2010**, *22*, 2155-2163. DOI:10.1021/cm9037796.
4. J. Diwu, A.-G. D. Nelson, S. Wang, T. E. Albrecht-Schmitt, "Comparison of Pu(IV) and Ce(IV) Diphosphonates," *Inorganic Chemistry*, **2010**, *49*, 3337-3342. DOI:10.1021/ic100184q.
3. A.-G. D. Nelson, T. E. Albrecht-Schmitt, "Unusual Case of a Polar Copper(II) Uranyl Phosphonate that Fluoresces," *Comptes Rendus Chimie*, **2010**, *13*, 755-757. *Invited article.* DOI:10.1016/j.crci.2010.03.011.
2. J. Diwu, A.-G. D. Nelson, T. E. Albrecht-Schmitt, "Using Phosphonates to Probe Structural Differences between Transuranium Elements and Their Proposed Surrogates," *Comments on Inorganic Chemistry*, **2010**, *31*, 46-62. *Invited Article.* DOI:10.1080/02603590903519988.
1. S. Wang, E. V. Alekseev, J. Ling, S. Skanthakumar, L. Soderholm, W. Depmeier, T. E. Albrecht-Schmitt, "Neptunium Diverges Sharply from Uranium and Plutonium in Crystalline Borate Matrixes: Insights into the Complex Behavior of the Early Actinides Relevant to Nuclear Waste Storage," *Angewandte Chemie*, *Int. Ed.*, **2010**, *49*, 1263-1266. *Selected for Cover Art Feature.* DOI:10.1002/anie.200906127.

Book Chapters

1. *Hydrothermal Synthesis and Crystal Structures of Actinide Compounds*, T. Albrecht-Schmitt, Peter C. Burns, and Sergey V. Krivovichev in *The Chemistry of the Actinide and Transactinide Elements*, **2010**.
2. J. Diwu and T. E. Albrecht-Schmitt, *Structural Chemistry of Transuranium Phosphonates in Metal Phosphonates*, A. Clearfield ed. **2011**, RSC.

Invited Lectures and Conference Talks at:

Florida State University, Oregon State University, University of Minnesota, Michigan State University, University of Kiel, Shangxi Normal University (China), Northwest University (China), University of Science and Technology of China, Chinese Institute of Atomic Energy, International Union of Crystallography Meeting (Madrid), Rare Earth Research Conference (session organizer), Plutonium Futures (plenary lecture). My students gave a number of lectures at ACS meetings. My student Shuao Wang was awarded the best poster award at Plutonium Futures and he won an ACS Young Investigator Award.

Recent Results

Rather than summarizing or highlighting all of the above works, results are presented on the remarkably complex transuranium borate system that is summarized in part from publications 47 and 28 (from selected publications); the former was a mini-review. This work combines aspects of fundamental studies on reactivity, structure, and bonding.

Introduction to Actinide Borates

The terrestrial abundance of boron, mostly existing as borates, is approximately 10 ppm.[1] Large borate deposits occur as the result of the evaporation of ancient oceans and seas. Uranium, the heaviest naturally occurring element, has a relatively low terrestrial abundance at 2.7 ppm.[2] However, a variety of processes concentrate uranium in the Earth's crust, and numerous uranium minerals with most of the common oxo-anions have been discovered.[3-5] Surprisingly, borate and uranium deposits have never been found to co-exist, and there are no known uranium borate minerals. However, the disposal of nuclear waste results in large amounts of actinides from uranium to curium and borates being artificially concentrated together for the first time.

Except for Russia, which has produced aluminophosphate glasses for decades, borosilicate glasses have become the only waste form for high-level radioactive waste.[6,7] In the United States, the vitrification of nuclear waste using borosilicate glasses started in 1996 primarily at the Savannah River Site, and this process is estimated to continue for at least two decades to vitrify the waste associated with the production of plutonium for nuclear weapons.[8] It has been recognized that both processing techniques and high actinide content in the glasses can lead to the formation of crystalline products such as silicates and borates within these glasses, which may lower the chemical durability and the integrity of the glass.[7,8]

One of the well-known salt deposits is the Salado formation near Carlsbad, New Mexico where the concentration of borate, predominately in the form of H_3BO_3, $B(OH)_4^-$, and $B_4O_7^{2-}$ reaches concentrations as high as 166 ppm in intergranular brines.[9] Located within this deposit is the United States' only repository for nuclear defense waste known as the Waste Isolation Pilot Plant (WIPP). WIPP presents a unique environment whereby large quantities of not only uranium, but also lesser amounts of the transuranium elements neptunium, plutonium, americium, curium, will eventually be able to react with the brines, potentially leading to the formation of actinide borate compounds. Recent complexation and speciation studies of neodymium(III), which acts as a surrogate of An(III) (An = actinide) in simulated WIPP brines have shown that borate competes with carbonate for An(III) complexation under the repository conditions.[10] The presence of the decaying nuclear waste will lead to heating beyond the ambient conditions in the deposit, and therefore the reactions of actinides with borates at moderate

temperatures are important reactions to study in order to predict the fate of actinides in the repository.

Finally, the recent earthquake and tsunami in Japan that crippled the *Fukushima Daiichi* nuclear power plant caused the release and dispersion of radioactive materials. In an effort to prevent the nuclear fuel rods from melting down, large amounts of sea water and boric acid were pumped into the reactors. It appears that the cladding of the fuel rods failed, exposing the hot fuel to concentrated boric acid. As a result, actinides potentially reacted with borates to yield actinide borates.

Despite the importance of understanding all these mechanisms for forming actinide borates, there are very few examples of well-characterized actinide borates. In fact, until very recently there were no examples of transuranium borates. The first crystalline actinide borate compound reported was $K_6[UO_2\{B_{16}O_{24}(OH)_8\}]\cdot 12H_2O$, which was crystallized via the room temperature evaporation of water.[11] This compound adopts a complicated molecular structure consisting of a uranyl core surrounded by a 16-borate ring.[11] From 1986 to 1991, Gasperin synthesized seven actinide borate compounds, including $UO_2(B_2O_4)$, $Li(UO_2)BO_3$, $Na(UO_2)BO_3$, $Ca(UO_2)_2(BO_3)_2$, $Mg(UO_2)B_2O_5$, $Ni_7(UO_2)(B_4O_{14})$, and ThB_2O_5 by using molten B_2O_3 as a flux in high temperature (>1000 ºC) reactions.[12-18] These actinide borates contain BO_3 triangles, except for $Ni_7(UO_2)(B_4O_{14})$, which contains both BO_3 triangles and BO_4 tetrahedra.[16] No new actinide borates were reported for almost 20 years. More importantly, no actinide borates were synthesized at slightly elevated temperatures. One of the reasons is that the crystallization of actinide borate compounds can be greatly affected by the hydrolysis of actinides in solution.[19]

Uranyl Borates

Molten boric acid flux reactions have proven to be a safe and facile way to prepare actinide borate compounds. Particularly, the boric acid flux reactions of uranyl nitrate with alkali metal or pseudo alkali metal (Ag^+ and Tl^+) nitrates have already generated more than 37 novel uranyl borate compounds by simply changing the reaction conditions including the reaction temperature, reaction time, and stoichiometry of starting materials.[20-24] Further incorporation of the F^- anion in the starting materials can lead to a novel uranyl fluoroborate family.[25] Moreover, by adopting methyl boronic acid as an alternative flux which has a lower melting point, the first actinide boronate with the formula of $UO_2(CH_3BO_2)(H_2O)$ has been prepared.[26]

Topological classifications of the structures of the novel uranyl borates family

All uranyl borates we obtained to date are based on uranyl polyborate sheets. These sheets are formed by the corner condensation of BO_4 tetrahedra and BO_3 triangles. An example of such an arrangement for a typical uranyl borate is shown in Figure 1. This is a polyborate sheet observed in the structure of $Rb_2[(UO_2)_2B_{13}O_{20}(OH)_5]$,[23] and presented in skeletal and polyhedral modes in Figures 1a and 1b, respectively. The uranyl cations reside in the triangular holes within the polyborate sheets. It is possible to classify the type of these sheets based on the super triangle-like groups linked via BO_3 triangles selected within dashed red circle. The super-triangles are based on three BO_4 tetrahedra in the structure of

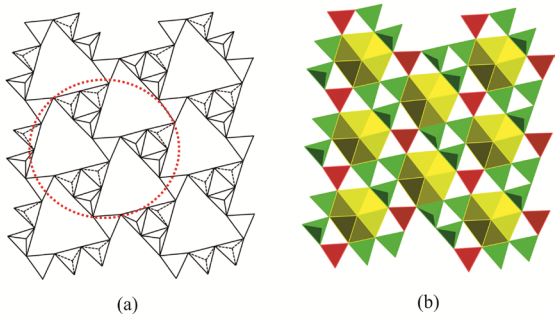

Figure 1. Skeletal (a) and polyhedral (b) representations of the polyborate sheet.

$Rb_2[(UO_2)_2B_{13}O_{20}(OH)_5]$ and in several other compounds. However, one of the borate units within super-triangle can be substituted by BO_3 triangles in other uranyl borate phases. Thus, the ratio between BO_3 and BO_4 units within the polyborate sheets is a key feature of the structural diversity that allows many possible types of polyborate sheets with similar topologies in actinide borate phases.

The coordination environment around the uranyl cation within the sheets can also be used to classify the sheet type. Typically, each uranyl cation is surrounded by nine neighbouring borate units (Figure 1b). Different types of sheets can be achieved by different numbers of BO_3 triangles and BO_4 tetrahedra and their coordination arrangements around the uranyl cations. For example, in the uranyl polyborate sheets of $Rb_2[(UO_2)_2B_{13}O_{20}(OH)_5]$, there are six BO_4 tetrahedra and three BO_3 triangles around each uranyl cation. Based on these aspects, up to date we have observed 11 different sheets types for all actinide borate compounds (Figure 2, types A-M) that are further complicated by the fact that many are enantiomorphic, and therefore sheet A also has an enantiomer A'.

For a typical uranyl borate, there are additional borate units that extend perpendicular to the planes of uranyl borate polyborate sheets to form a layered structure, or these borate units bridge between sheets to form a three-dimensional framework structure. A structural hierarchy based on the sheet extending and bridging is also observed in actinide borates. For example, in the Tl-uranyl borate system, the extending BO_3 triangles are tuning the structures by forming single layers, doubled layers, and 3D frameworks. This feature makes actinide borates unique among all known actinide systems.

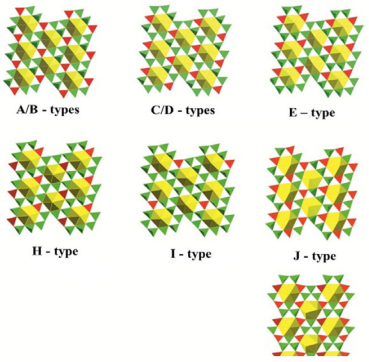

Figure 2. Polyhedral representations of all polyborate sheet types found to date in the actinide borate system.

The structural features and interrelationships of this large group of materials can be represented by lithium and silver uranyl boartes. Both lithium and silver uranyl borate families are represented only by single phases - $Li[UO_2B_5O_9]\cdot H_2O$ and $Ag[(UO_2)B_5O_8(OH)_2]$.[23] They are closely related in chemical composition and in structural aspects despite the large difference in ionic radii between Li^+ and Ag^+. The crystal structure fragments of Li and Ag uranyl borates are shown in Figure 3a and 3b, respectively. Both phases are based on the same **G**-type of polyborate sheets (Figure 2). There are additional BO_3 triangles extending perpendicular to the uranyl borate sheets in

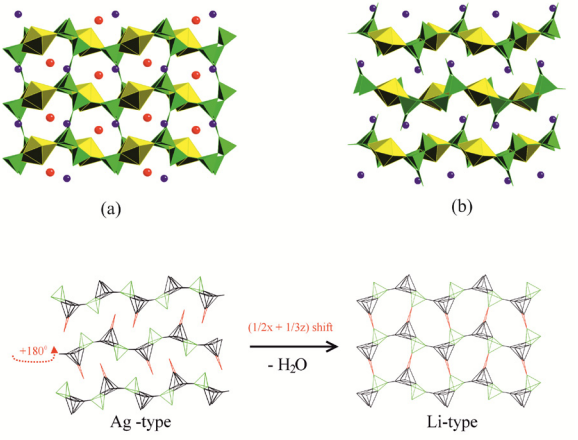

Figure 3. The crystal structures of $Li[(UO_2)B_5O_9]\cdot H_2O$ (a), $Ag[(UO_2)B_5O_8(OH)_2]$ (b) (UO_8 hexagonal bipyramids are shown in yellow, BO_3 and BO_4 units in green, Li and Ag cations in purple and water molecules in red) and schematic representation of $Li[(UO_2)B_5O_9]\cdot H_2O$ and $Ag[(UO_2)B_5O_8(OH)_2]$ structure type relationships (c).

these structures. However, they play different roles in Li and Ag uranyl borates. In the structure of the lithium phase, BO_3 triangles link uranyl borate sheets into a 3D framework, but in the structure of the silver phase they do not. The positions of lithium and silver cations are similar, and they reside between the sheets. There is enough space for water molecules to be present in the structure of $Li[UO_2B_5O_9]\cdot H_2O$ because of the small size of Li cations; while in the silver phase water molecules are absent. The relationship between described structure types is schematically presented in Figure 3c. The skeletal representations of polyborate nets in the Ag and Li structure types have been plotted in this Figure 3c. In order to transform the structures from the Ag-type to Li-type, we need to turn each second layer by 180° in the plane of the sheets (shown by red dashed arrow), and shift these sheets by translations of 1/2 in x and 1/3 in z. As a result of these manipulations the BO_2OH triangles (shown in red) will occupy positions that are very close to the BO_3OH tetrahedra (shown in red).

Neptunium Borates

As the first transuranium element, neptunium is extremely important because its main isotope ^{237}Np has a long half-life ($t_{½} = 2.14 \times 10^6$ years), and in the long-term will be the primary contributor to the calculated dose from spent nuclear fuel stored in repositories.[27] Neptunium can exist in the natural environment in oxidation states of IV, V, and VI; although neptunium under strongly oxidizing or reducing condition can really range from III to VII.[28] Np(V) is the most stable oxidation state in solution under most common conditions.[28] However, it is known that Np(V) will disproportionate to Np(VI) and Np(IV) under a variety of situations.[28] The relative stabilities between these oxidation states can be significantly affected by numerous factors such as concentration,[29] temperature,[30] counter ions,[31] radiolysis,[32] and hydrolysis.[19] A significant numbers of known neptunium compounds are mixed-valent containing Np(IV)/Np(V) or Np(V)/Np(VI).[33-37]

Borate is favorably endowed with the ability to coordinate with neptunium metal centers in all possible oxidation states for several reasons. First, the building units of borates, BO_3 triangles and BO_4 tetrahedra tend to polymerize under a variety of conditions to form countless types of polyborate anions which provides numerous bonding modes to possibly coordinate the metal centers with a variety of geometric requirements.[38-42] Second, borate itself is a non-redox-active ligand under most conditions. This provide us an opportunity of controlling or at least predicting the oxidation states of actinides in products by controlling the oxidation states of actinides and the reduction potentials in the starting materials. Herein we will discuss how we synthesized neptunium borates with mixed/intermediate or single valence states.

Mixed/intermediate-valent neptunium borates

When Np(VI) nitrate reacts with molten boric acid in the presence of K^+ or Ba^{2+} at 220 ºC, two highly unusual mixed/intermediate neptunium borate compounds, $K_4[(NpO_2)_{6.73}B_{20}O_{36}(OH)_2]$ and $Ba_2[(NpO_2)_{6.59}B_{20}O_{36}(OH)_2]\cdot H_2O$ are isolated.[24] These two compounds contain Np(IV), Np(V), and Np(VI) simultaneously, which serve as the first examples of actinide compounds containing three oxidation states for an actinide element, although several rare compounds containing transition metal elements were known to possess three oxidation states for a same element.[43,44] When Np(V) chloride was used as the starting material, where chloride and borate are the only counter ions in the reaction, $(NpO_2)_4[(NpO_2)_{6.73}B_{20}O_{36}(OH)_2]$ forms, which also contains Np(IV), Np(V), and Np(VI). Based on comparative studies using Np(VI) and Np(V) as the source of neptunium in these syntheses, it

has been determined that this compound forms by partial disproportionation of the Np(V) to yield Np(VI) and Np(IV). The fact that this compound forms with many different interlayer cations and from different oxidation states of neptunium suggests that it represents an energetic well.

The structures of $K_4[(NpO_2)_{6.73}B_{20}O_{36}(OH)_2]$ and $Ba_2[(NpO_2)_{6.59}B_{20}O_{36}(OH)_2]\cdot H_2O$ are highly complicated as shown in Figure 4a. The overall structure is layered with slabs of neptunyl borate separated by K^+ or Ba^{2+} cations. These neptunyl borate layers are based on two sub-layers and approximately 1.6 nm thick which is much thicker than other layered actinide compounds. Within the neptunyl borate layers, there are four distinct neptunium sites. In all cases the neptunium is found in the form of an approximately linear dioxo cation, NpO_2^{n+}. In two of the sites the NpO_2^{n+} cations are coordinated by six oxygen atoms in the equatorial plane to form an NpO_8 hexagonal bipyramid. One NpO_2^{n+} cation is bound by five oxygen atoms to form an NpO_7 pentagonal bipyramid. Bond-valence sum calculations suggest the NpO_8 units being primarily +6 and the NpO_7 units primarily +5. The final NpO_2^{n+} cation is bonded to four oxygen atoms in equatorial plane to yield a tetragonal bipyramid. The core neptunyl unit in this position has Np=O bond distances that average 1.938(14) Å, which are considerable longer than those found in Np(V) compounds, which average 1.83(2) Å. The neptunyl bond distances and the bond-valence sum calculations indicate Np(IV). More importantly, the NpO_6 site is solely held in place by so-called *cation-cation interactions* which describe the scenario that the "yl" oxo atoms from one neptunyl cation bond to a neighboring neptunium polyhedron in its equatorial plane.[45,46] Not only dioxo Np(IV) unit, but also this CCI-only surrounding coordination environment, were observed for the first time in these compounds. All together, the joining of the NpO_6, NpO_7, NpO_8, BO_3, and BO_4 units creates the remarkable neptunyl borate layers. The length of this "yl" unit varies with the type of interlayer cation. When K^+ is in the interlayer space the distances are closer to that found with Np(V). When NpO_2^+ is in the interlayer space the neptunium site is holosymmetric with a normal octahedral environment for Np(IV). It has been suggested to us that the strange 1.938(14) Å distance represents crystallographic averaging of Np(V) and Np(IV) sites, and this may well be the case.

The UV-vis-NIR spectroscopy measurements taken from crystals of $K_4[(NpO_2)_{6.73}B_{20}O_{36}(OH)_2]$ and $Ba_2[(NpO_2)_{6.59}B_{20}O_{36}(OH)_2]\cdot H_2O$ provided much stronger evidences for the existence of three oxidation states for neptunium in these crystals. Absorption features are present that clearly identify Np(IV), Np(V), and Np(VI) as shown in Fig. 4b. The most important f-f transitions for Np(IV) are the transitions near 700 nm and 800 nm; whereas the Np(V) and Np(VI) transitions are observed near 990 and 1200 nm, respectively.[47] Based on the comparison of the electronic spectroscopy and the crystal structure, the following formula based on formal oxidation states could be proposed, $K_4[(Np^{IV}O_2)_{0.73}(Np^{V}O_2)_2(Np^{VI}O_2)_4B_{20}O_{36}(OH)_2]$ and $Ba_2[(Np^{IV}O_2)_{0.59}(Np^{V}O_2)_2(Np^{VI}O_2)_4B_{20}O_{36}(OH)_2]\cdot H_2O$. Calculations based on the known

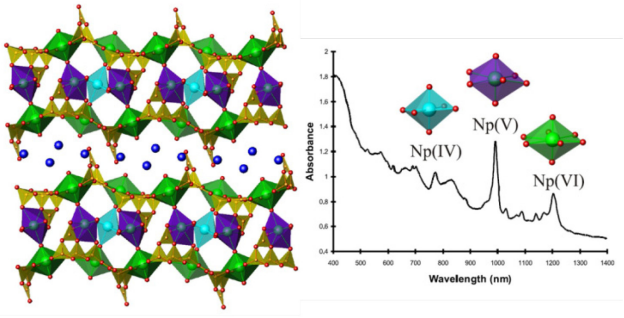

(a) (b)

Figure 4. A depiction of the structure of $K_4[(NpO_2)_{6.73}B_{20}O_{36}(OH)_2]$ or $Ba_2[(NpO_2)_{6.59}B_{20}O_{36}(OH)_2]\cdot 0.6H_2O$ showing $Np^{VI}O_8$ (green), $Np^{V}O_7$ (dark blue), and $Np^{IV}O_6$ (light blue) units linked by BO_3 triangles and BO_4 tetrahedra (a) and UV-vis-NIR spectrum of $K_4(NpO_2)_{6.73}B_{20}O_{36}(OH)_2$ showing regions of f-f transitions that indicate the presence of Np(IV), Np(V), and Np(VI) (b).

extinction coefficients and the measured of the intensities of the primary peaks in the UV-vis-NIR spectrum are consistent with this formulation.

The magnetic susceptibility measurement for the $K_4[(NpO_2)_{6.73}B_{20}O_{36}(OH)_2]$ show the sample to be simply paramagnetic down to the lowest temperature measured. Fitting the susceptibility data assuming Curie-Weiss behavior of non-interacting, localized moments, produces an effective moment of 3.08 ± 0.15 μ_B per Np ion. The theoretical, free-ion effective moments, based on Russell Saunders coupling, are 3.62, 3.58, and 2.54 μ_B for Np(IV), Np(V), and Np(VI), respectively.[48] It is interesting that if the susceptibilities are calculated assuming the free-ion moments weighted by the ratios of crystallographic multiplicities, yields a calculated effective moment of 3.01 μ_B per Np ion, well within the error of the experiment. The presence of neptunyl (V) and/or (IV) is confirmed by these results because these valence states are required to increase the measured value above the 2.54 μ_B theoretical value for Np(VI). This behavior is similar to the mixed-valent Np(IV)/Np(V) selenite, $Np(NpO_2)_2(SeO_3)_3$,[33] and contrasts sharply with most pure Np(V) compounds that either ferromagnetically order <10 K or antiferromagnetically order near 20 K.[49,50]

Neptunium(VI) borate

The counter anions present in the starting materials for making neptunium borates are found to be the key factor for controlling the oxidation states of neptunium in the final products. When nitrate or chloride is present in the boric acid flux reactions, mixed/intermediated valent neptunium borates are always isolated.[24,51] When an oxidative-active anion, perchlorate is used in the reaction, i.e., Np(VI) perchlorate is used as starting material, a Np(VI) borate, $NpO_2[B_8O_{11}(OH)_4]$ can be successfully synthesized.[52]

Single crystal X-ray diffraction study on $NpO_2[B_8O_{11}(OH)_4]$ shows that this compound adopts a noncentrosymmetric framework structure crystallized in the space group *Cc*. A view of the overall structure is shown in Figure 5a. There is one crystallographically unique neptunyl cation, NpO_2^{2+}, that resides in a hexagonal hole within the polyborate sheets to create a hexagonal bipyramidal environment, AnO_8. Each AnO_8 unit is surrounded by nine borate groups in [*ac*] plane to form an actinyl borate sheet. The sheet topology which is named as the H-Type (Figure 2) is unique among all actinide borates that we have observed. There are additional BO_3 triangles and BO_4 tetrahedra connecting these actinyl borate sheets together to form the framework structure. It should be noted that this is the only actinyl borate structure type from boric acid reactions where BO_4 tetrahedra are located between the sheets. The twisting of the interlayer borate groups with respect to one another reduces the interlayer space, and yields a less open, denser structure.

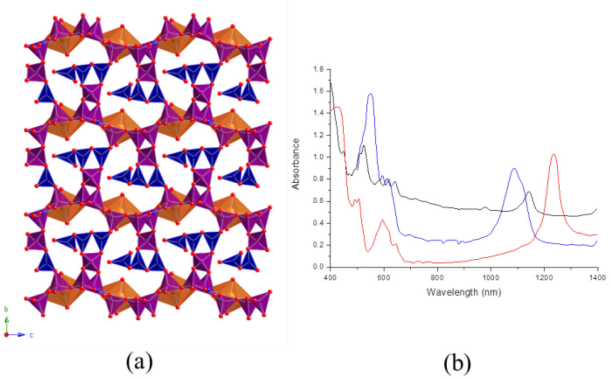

Figure 5. (a) A depiction of the polar, three-dimensional network found for $NpO_2[B_8O_{11}(OH)_4]$. NpO_8 hexagonal bipyramids are shown in orange, BO_3 triangles in blue, and BO_4 tetrahedra in purple. (b) UV-vis-NIR absorption spectra of the Np(VI) compounds, $NpO_2[B_8O_{11}(OH)_4]$ (black), $NpO_2(NO_3)_2{\cdot}6H_2O$ (blue), and $NpO_2(IO_3)_2(H_2O)$ (red).

The U(VI) and Pu(VI) analogue of $NpO_2[B_8O_{11}(OH)_4]$ can also be made. Thus, the actinide contraction in this series of compounds $AnO_2[B_8O_{11}(OH)_4]$ (An = U, Np, Pu) can be demonstrated with a variety of metrics. First, the unit cell volumes for $UO_2[B_8O_{11}(OH)_4]$, $NpO_2[B_8O_{11}(OH)_4]$, and $PuO_2[B_8O_{11}(OH)_4]$ are 1183.4(5) $Å^3$, 1182.1(2) $Å^3$, and 1180.0(3) $Å^3$, respectively, nicely fit the order of the actinide contraction. More importantly the actinyl An≡O bond distances shrink by 0.02 Å on average from uranium to plutonium. It is important to note that actinyl bonds distances are close enough to each other across the uranium, neptunium, and plutonium series that the actinide contraction is difficult to detect between different types of compounds (i.e. the errors in the bond lengths produce overlap if one uses 3σ on the calculated errors). The actinide contraction is only detectable if the errors are small, the residuals are low, and the compounds are isostructural.[53]

The $5f^1$ electron configuration typically yields a single somewhat broad Laporte-forbidden f-f transition in addition to higher energy charge-transfer bands.[54] For U(V) the f-f transition is in the visible region of spectrum.[54] For isoelectronic Np(VI), this transition occurs in the NIR near 1200 nm. The UV-vis-NIR spectra of $NpO_2[B_8O_{11}(OH)_4]$ acquired from a single crystal is shown in Figure 5b. We have found that this peak can be shifted from where it typically occurs in solution when compared to solid samples. For example, data acquired from single crystals of $NpO_2(NO_3)_2{\cdot}6H_2O$ shows this peak is located at 1100 nm. $NpO_2[B_8O_{11}(OH)_4]$ shows a transition at 1140 nm. In contrast, in single crystals of $NpO_2(IO_3)_2(H_2O)$ the transition is at 1230 nm, which is similar to where it is found in perchlorate and nitrate solutions.[47] Moreover, this transition found in $KNpO_2PO_4{\cdot}3H_2O$ is at 1427 nm. An explanation for the differences in the energy of this transition is the coordination environments of Np(VI). In $NpO_2[B_8O_{11}(OH)_4]$ and $NpO_2(NO_3)_2{\cdot}6H_2O$ the neptunium center is in a hexagonal bipyramidal environment. In $NpO_2(IO_3)_2(H_2O)$ and solutions of neptunyl perchlorate the neptunium is in a pentagonal bipyramidal geometry.[55] In $KNpO_2PO_4{\cdot}3H_2O$, a tetragonal bipyramidal geometry is found for Np(VI).[56] It appears that the addition of a larger number of donor atoms in the equatorial plane, and presumably more electron density at the neptunium center, shifts the f-f transition to higher energy. The reverse effect is observed in the shift of the main transition at 980 nm in Np(V) compounds. Upon the formation of cation-cation interactions, the f-f transition shifts to longer wavelengths.[46]

Plutonium Borates

Plutonium is a highly unusual element, perhaps the most complex in the periodic table, and its chemistry in both aqueous solution and in the solid state are very rich.[57] Five oxidation states including Pu(III), Pu(IV), Pu(V), Pu(VI), and Pu(VII) are accessible in aqueous solution and can be prepared in solid state under the appropriate conditions.[57] The redox chemistry of plutonium is very complicated due to the fact that Pu(III), Pu(IV), Pu(V), Pu(VI) can coexist in solution under a wide range of conditions.[57] Although neptunium in both aqueous solution and solid state is dominated by Np(V) species,[28] several mixed/intermediate valence neptunium borate compounds can still be prepared in boric acid flux as discussed above. It is thus expected that mixed/intermediate-valent plutonium borates can be prepared. However, only monovalent plutonium borates including Pu(VI) and Pu(III) borates can be made when plutonium in single oxidation state is used as the starting material.[52,58]

Plutonium(VI) borate

The boric acid flux reaction of Pu(VI) nitrate leads to the formation of the first Pu(VI) borate compound, $PuO_2[B_8O_{11}(OH)_4]$. As mentioned above, this compound is part of the isotypic series $AnO_2[B_8O_{11}(OH)_4]$ (An = U, Np, Pu). $PuO_2[B_8O_{11}(OH)_4]$ can also crystallizes in the presence of Ba^{2+} and K^+.[52] However, unlike uranyl and neptunyl borates, additional cations are not readily incorporated into the structure. More importantly, in effort to make a Pu(IV) borate compound, where Pu(IV) nitrate starting materials was used, the same Pu(VI) borate compound $PuO_2[B_8O_{11}(OH)_4]$ was isolated. The isolation of a Pu(VI) borate from a Pu(IV) source is surprising in light of the fact that Pu(IV) compounds are generally far less soluble and more stable than Pu(VI) compounds.[57]

The first twelve years of my career as a professor have been largely focused on working with actinides in the +4, +5, and +6 oxidation states. We intentionally avoided +3 because 1) Pu(III) is air-sensitive, and we had not yet developed techniques for working with air-sensitive transuranics, 2) ^{243}Am is highly radioactive and we needed new techniques for working with an isotope that is this short-lived, 3) ^{248}Cm is extremely scarce and hard to obtain, 4) ^{249}Cf is even harder to obtain than ^{248}Cm, and has very penetrating γ radiation, and finally and most importantly, 5) I believed (incorrectly) that the trivalent actinides would be identical to lanthanides. The decision to solve problems 1-5 has resulted in what I believe to be the best work of my career, and I have four graduate students now dedicated to carrying out this work.

The similarities between the trivalent lanthanides and actinides is ascribed to the fact that their valence 4f and 5f orbitals are primarily nonbonding, and these Ln^{3+} and An^{3+} cations can possess nearly identical ionic radii that both follow the well-established contractions across the series.[59,60] This ostensibly identical chemistry has been developed in great detail for the aqua ions, e.g. $[Ln(H_2O)_9]^{3+}$ and $[An(H_2O)_9]^{3+}$, where both theory and experiment confirm that the structures are isotypic, the f orbitals are nonbonding, and the only changes that are observed occur as function of the ionic radius of the metal ions.[61] The correlations between the chemistries of these two series creates a significant technological hurdle in the recycling of used nuclear fuel where it is necessary to separate trivalent lanthanide fission products that can act as neutron poisons from Am^{3+} and Cm^{3+}; the latter can be recycled and utilized for energy production or fissioned for waste mitigation.[62]

Previous reports on rare earth borates have focused on preparing lanthanide borates by reacting lanthanide oxides with boric acid either as a flux[63] or under hydrothermal conditions.[64] The flux reactions yielded hexaborates, $H_3LnB_6O_{12}$ (Ln = Sm − Lu), pentaborates, $Ln[B_5O_9]$ (Ln = Sm − Lu), octaborates, $Ln[B_8O_{11}(OH)_5]$ (Ln = La − Nd), and nonaborates, $Ln[B_9O_{13}(OH)_4]\cdot H_2O$ (Ln = Pr − Eu);[63] whereas the hydrothermal syntheses afforded $Ln_2[B_6O_{10}(OH)_4]\cdot H_2O$ (Ln = Pr, Nd, Sm − Gd, Dy, Ho, and Y).[64]

Structure and Topology Description.

Lanthanides: $Ln[B_4O_6(OH)_2Cl]$. The reaction of the lanthanide/actinide chlorides and boric acid is a facile method for the production of f-element polyborate compounds. The early lanthanides result in the formation of $Ln[B_4O_6(OH)_2Cl]$ (Ln = La − Nd), which crystallize in the noncentrosymmetric, monoclinic space group, *Cc*. The praseodymium and neodymium compounds have previously been reported,[65] but the lanthanum and cerium analogues are a result of our work.

$$LnCl_{3(s)} + 4H_3BO_{3(s)} \rightarrow Ln[B_4O_6(OH)_2Cl]_{(s)} + 4H_2O_{(l)} + 2HCl_{(g)} \quad (Ln = La - Nd) \quad \textbf{(1)}$$

These compounds form dense, three-dimensional structures as shown in Figure 6a and contain only corner-sharing BO_3 and BO_4 units, which create triangular holes (where each edge composed of two BO_4 tetrahedra and one BO_3 triangle) where the rare earth cations reside. The sheet topology (Figure 6b) found in these structures is very similar to those found with penta- and hexavalent actinides (e.g. U(VI), Np(V), Np(VI), and Pu(VI)).[20-26,51,52,58]

The polyborate sheet topology provides six oxygen donors that are nearly co-planar forcing a ten-coordinate geometry not typically found for trivalent lanthanides or actinides. This ten-coordinate geometry (Figure 7a) is best described as a capped triangular cupola,[66] where the capping group is a chloride anion, and the triangular base is composed of oxygens from two different BO_4 groups and an additional chloride anion. Furthermore, the chloride anions bridge between metal centers, and these bridges span between the sheets. This type of connectivity is absent in nearly all of the lanthanide and actinide borates that have been prepared.

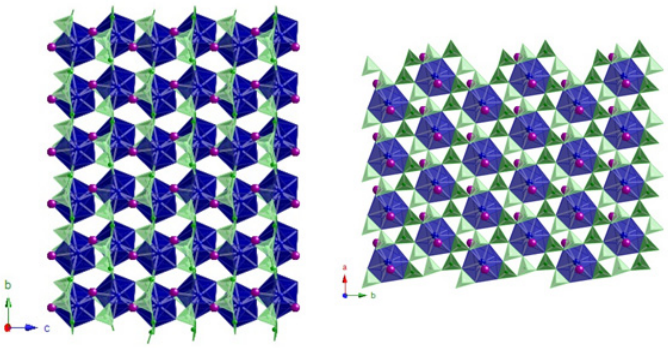

Figure 6. Depiction of the (a) three-dimensional framework and (b) sheet topology of $Ln[B_4O_6(OH)_2Cl]$ (Ln = La − Nd; Pu). The lanthanide and plutonium metal centers are depicted by the blue spheres, chlorine is depicted by the purple spheres, BO_4 tetrahedra as light green unit, and BO_3 triangles as dark green units.

$Ln_4[B_{18}O_{25}(OH)_{13}Cl_3]$. Samarium and europium both represent a transition point in the lanthanide series. The product obtained from these lanthanides is $Ln_4[B_{18}O_{25}(OH)_{13}Cl_3]$ (Ln = Sm, Eu), which crystallizes in the monoclinic space group, *P*2/*c*.

$$8LnCl_{3(s)} + 36H_3BO_{3(s)} \rightarrow 2Ln_4[B_{18}O_{25}(OH)_{13}Cl_3]_{(s)} + 32H_2O_{(l)} + 18HCl_{(g)} \quad (Ln = Sm - Eu) \quad \textbf{(2)}$$

These materials also form dense, but different, three-dimensional structures, as well as a different sheet topology. Like $Ln[B_4O_6(OH)_2Cl]$ (Ln = La− Nd) , corner-sharing BO_3 and BO_4 units create triangular holes (also composed of two BO_4 tetrahedra and one BO_3 triangle), which provide residence for the metal center. The $Ln_4[B_{18}O_{25}(OH)_{13}Cl_3]$ product is not only novel for the lanthanides but also for the actinides.

The metal centers in this structure are either bridged or terminal, but all possess an unusual nine-coordinate hula-hoop geometry.[67] Like the $Ln[B_4O_6(OH)_2Cl]$ (Ln = La − Nd) structure, the polyborate network provides six oxygen atoms that are nearly co-planar, and the additional ligands are two oxygen

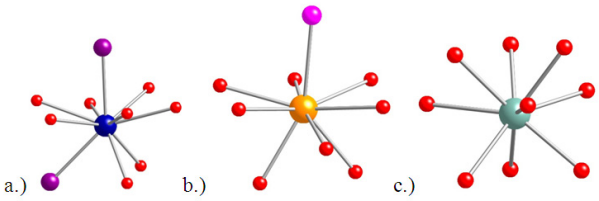

Figure 7. Coordination geometries for the lanthanide and actinide metal centers. (a) Capped triangular cupola (b) hula hoop (c) tricapped trigonal prism.

atoms from either two BO_4 groups (bridging) or one oxygen from a BO_3 group and a hydroxide (non-bridging). This chloride bridge is similar to that observed in $Ln[B_4O_6(OH)_2Cl]$ (Ln = La− Nd) though $Ln_4[B_{18}O_{25}(OH)_{13}Cl_3]$ (Ln = Sm, Eu) contain only one bridging, apical chloride.

$Ln[B_6O_9(OH)_3]$. The structures and local coordination environment of $Ln[B_6O_9(OH)_3]$ (Ln = Y, Eu− Lu) have been reported elsewhere.[63a,b] However, our study has found that yttrium, which is generally regarded as an honorary lanthanide, forms the $Ln[B_6O_9(OH)_3]$ structure type as well. It should be noted the exclusion of chloride from the inner coordination sphere, a change in geometry to a more typical tricapped trigonal prism, and crystallization in the rhombohedral space group, *R*3*c* is observed with the smaller lanthanides.

$2LnCl_{3(s)} + 12H_3BO_{3(s)} \rightarrow 2Ln[B_6O_9(OH)_3]_{(s)} + 12H_2O_{(l)} + 6HCl_{(g)}$ (Ln = Eu – Lu, Y) **(3)**

Trivalent Actinides. $Pu[B_4O_6(OH)_2Cl]$. As the redox chemistry for plutonium is much more complex than any of the lanthanides, strict anaerobic conditions are required in order to obtain trivalent plutonium borates. Pu(III) yields two different products. The first and major product, $Pu[B_4O_6(OH)_2Cl]$ (**PuBOCl-1**), is isotypic with $Ln[B_4O_6(OH)_2Cl]$ (Ln = La − Nd).

$PuCl_3(s) + 4H_3BO_3(s) \rightarrow Pu[B_4O_6(OH)_2Cl](s) + 4H_2O(l) + 2HCl(g)$ **(4)**

The structure, sheet topology, and local coordination environment discussions are discussed above and shown Figure 6.

$Pu_2[B_{13}O_{19}(OH)_5Cl_2(H_2O)_3]$. The second trivalent plutonium borate, $Pu_2[B_{13}O_{19}(OH)_5Cl_2(H_2O)_3]$ (**PuBOCl-2**), is the minor product (20%) of the reaction and is completely novel for the lanthanides and actinides. $Pu_2[B_{13}O_{19}(OH)_5Cl_2(H_2O)_3]$ crystallizes in the monoclinic space group $P2_1/n$ and does not have a lanthanide analogue.

$2PuCl_3(s) + 13H_3BO_3(s) \rightarrow Pu_2[B_{13}O_{19}(OH)_5Cl_2(H_2O)_3](s) + 12H_2O(l) + 4HCl(g)$ **(5)**

The three-dimensional framework, local coordination environment, and sheet topology (Figures 8a and 9a) of **PuBOCl-2** is completely different than those of $Ln[B_4O_6(OH)_2Cl]$ (Ln = La− Nd) or **PuBOCl-1**. **PuBOCl-2** contains Pu(III) in a ten-coordinate environment with the capped triangular cupola geometry (Figure 9a).

The polyborate network provides six oxygen atoms that are nearly co-planar, and the additional ligands are a capping chloride and a triangular base composed of a water molecule and oxygen atoms from two different BO_3 groups. The apical chloride in this compound is terminal and does not bridge to other metal centers. While triangular holes are still

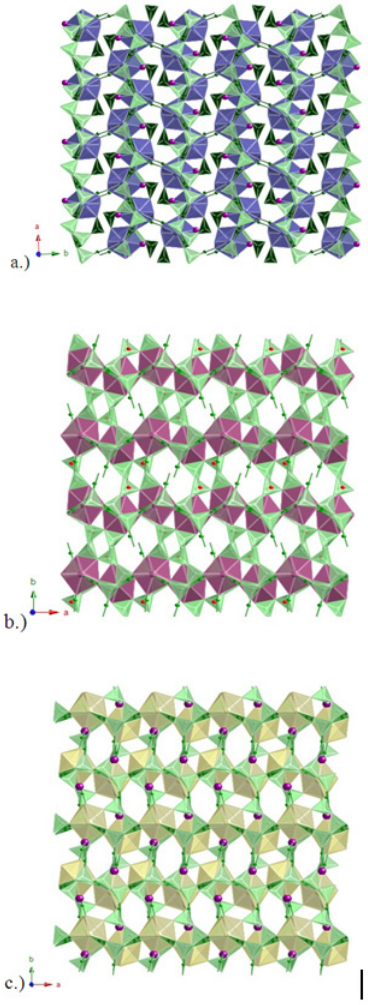

Figure 8. Three-dimensional framework structures of Pu(III), Am(III), and Cm(III) borates.

present in the sheet topology, the units making up the holes are two BO_3 triangles and one BO_4 tetrahedron. This is the complete opposite of what is observed in $Ln[B_4O_6(OH)_2Cl]$ (Ln = La – Nd; Pu). Additionally, the sheet topology contains a unit of three corner-sharing BO_4 tetrahedra connected via a μ_3-oxygen atom. For comparison, this sheet topology is also present in the $Ln[B_8O_{11}(OH)_5]$ (Ln = La − Nd) and $Ln[B_9O_{13}(OH_4)]\cdot H_2O$ (Ln = Pr − Eu) systems,[63c] but the three-dimensional framework is completely novel.

$Am[B_9O_{13}(OH)_4]\cdot H_2O$. The americium borate, $Am[B_9O_{13}(OH)_4]\cdot H_2O$ (**AmBO**), represents a transition in the actinide series as far as structure, coordination environment, and bonding is concerned. While **AmBO** crystallizes in the monoclinic space group $P2_1/n$ and has the same sheet topology as **PuBOCl-2,** minus the chloride moiety, its local coordination environment and three-dimensional network are completely different (Figures 8b and 9b). The most noticeable difference between **AmBO**, **PuBOCl-1**, and **PuBOCl-2** is the lack of chloride.

$$2AmCl_3(s) + 18H_3BO_3(s) \rightarrow 2Am[B_9O_{13}(OH)_4]\cdot H_2O(s) + 18H_2O(l) + 6HCl(g) \quad \textbf{(6)}$$

AmBO has the same nine-coordinate hula-hoop geometry (Figure 9b) as observed in the $Ln_4[B_{18}O_{25}(OH)_{13}Cl_3]$ (Ln = Sm, Eu) structures. The six nearly coplanar equatorial oxygen atoms come from the two BO_3 triangles and one BO_4 tetrahedron present in the sheet layer and create the triangular hole in which the americium atom resides. The additional oxygens come from one chelating BO_4 tetrahedra in the base and one BO_3 triangle in the capping position, which bridges to the layer above.

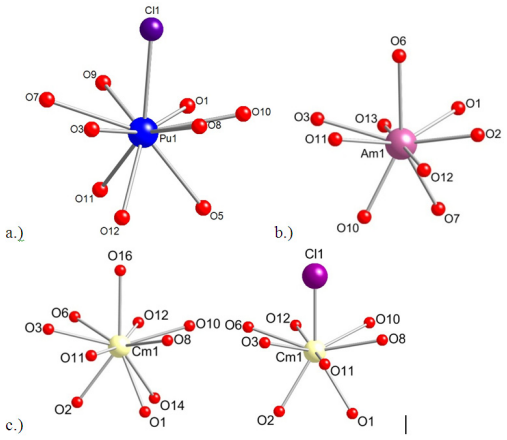

Figure 9. Coordination geometries and labeled bonds in (a) $Pu_2[B_{13}O_{19}(OH)_5Cl_2(H_2O)_3]$, (b) $Am[B_9O_{13}(OH)_4]\cdot H_2O$, and (c) $Cm_2[B_{14}O_{20}(OH)_7(H_2O)_2Cl]$. The actinide metal centers are depicted by blue (a), pink (b), or yellow (c) spheres, oxygens as red spheres, and chlorine as purple spheres.

$Cm_2[B_{14}O_{20}(OH)_7(H_2O)_2Cl]$. The curium borate, $Cm_2[B_{14}O_{20}(OH)_7(H_2O)_2Cl]$ (**CmBOCl**), is a unique structure in that it contains two distinct curium sites with different coordination geometries and is novel for both the lanthanides and actinides. The first site is a ten-coordinate capped triangular cupola with an oxygen atom in the capping position, and the second is a nine-coordinate hula-hoop with a terminal chloride in the apical position (Figure 9c). **CmBOCl** crystallizes in the monoclinic space group $P2_1/n$ and has the exact same sheet topolgy as **PuBOCl-2** and **AmBO**, but a completely different three-dimensional framework (Figure 8c). It is interesting to note the renewal of the chloride moiety even if on only half the curium sites.

$$2CmCl_3(s) + 14H_3BO_3(s) \rightarrow Cm_2[B_{14}O_{20}(OH)_7(H_2O)_2Cl](s) + 13H_2O(l) + 5HCl(g) \quad \textbf{(7)}$$

The ten-coordinate center in **CmBOCl** is capped by an oxygen atom from a BO_3 triangle, and the triangular base is composed of oxygens from one BO_3 group and two different BO_4 groups. The nine-coordinate center has a chloride as the capping group, and the two base sites are composed of oxygens from two different BO_4 groups.

Periodic Trends. From this study, it became evident that there are discontinuities in the resulting structure types that occur between the lanthanide and actinide borates. The lanthanides yield products that occur in blocks that depend on a) the presence/absence of the chloride and b) steric factors that correlate with changes in the ionic radii of these elements. Depending on the identity of the lanthanide, three different products were obtained in a high yield, which are given in Equations 1-3.

It is unfortunate that the ionic radii for Pu^{3+} and Cm^{3+} have never been determined beyond coordination number (CN) six and Am^{3+} beyond eight.[60] Thus, the highest value common between the lanthanides and actinides is six and will be used for comparisons henceforth. The first structure type that emerges from the lanthanides is $Ln[B_4O_6(OH)_2Cl]$ (Ln = La − Nd) where the trivalent ionic radii for these metals are 1.032, 1.01, 0.99, and 0.98 Å, respectively.[60] The second structure type, $Ln_4[B_{18}O_{25}(OH)_{13}Cl_3]$ (Ln = Sm, Eu), possesses metal centers with trivalent ionic radii of 0.958 and 0.947 Å, respectively, while the third structure type, which lacks the chloride entirely, $Ln[B_6O_9(OH)_3]$ (Ln = Eu – Lu, Y), possess metal centers with trivalent ionic radii of 0.947 to 0.861 Å, respectively.[60] It is of interest that yttrium belongs in the third structure type. With a trivalent ionic radius (CN = 6) of 0.900 Å, yttrium would fall roughly in between holmium and erbium.[60]

The actinide products, however, do not seem to depend on the presence/absence of the chloride or the ionic radii, but instead on the identity of the metal itself. Depending on the identity of the actinide, four different products were obtained and can be seen in Equations 4-7.

The ionic radii (CN = 6) for Pu^{3+}, Am^{3+}, and Cm^{3+} are 1.00, 0.975, and 0.970 Å, respectively.[60] Upon examination of the ionic radii, it would be expected, based solely upon purely ionic interactions, that plutonium should yield exclusively the $Ln[B_4O_6(OH)_2Cl]$ compound and americium and curium should yield the same compound yet intermediate of the **LaBOCl** and **SmBOCl** products. However, this expectation is not entirely realized. While the plutonium does indeed yield **PuBOCl-1**, which is isotypic with the **LaBOCl** product, it also produces a minor product of **PuBOCl-2** which is not observed in any of the lanthanide reactions or for any other actinide reaction to date.[68,69] **AmBO** lacks chloride entirely and is isotypic with the products obtained where the lanthanide oxides of Pr and NdEu are used as the starting material.[63a,b] The curium reaction, which was expected to yield the same product as the americium based solely on the ionic radii, produced $Cm_2[B_{14}O_{20}(OH)_7(H_2O)_2Cl]$ with two different curium sites.[69] The first site possesses a nine coordinate geometry and contains a chloride, while the other site lacks the chloride but is ten coordinate. This is a hybrid of what is observed in the plutonium and americium reactions. Also, this product, to date, is unique only to curium. It is of interest that the area of greatest structural change occurs for the congeners of each series (Sm-Gd for the lanthanides and Pu − Cm for the actinides).

The average An−O bond length in **AmBO** is 2.497 Å while the averages for **PuBOCl-1** and **PuBOCl-2** are 2.585 and 2.609 Å, respectively. This large difference in An−O bond lengths between the plutonium and americium borates can be attributed to a change in coordination environment, different structures, as well as a substantial change in ionic radii. The average bond length in **CmBOCl** is 2.557 and 2.590 Å for the nine and ten-coordinate species, respectively. These averages fall roughly in the middle of what is observed in **PuBOCl-1**, **PuBOCl-2**, and **AmBO**, which is to be expected as **CmBOCl** has bonding and coordination environments of both the plutonium and americium borates.

Under the Pearson definition of hard/soft acids and bases, the lanthanides and actinides are considered hard acids while chloride is a soft base.[70] This line of thought nicely explains the trend of all bridging, to half bridging, to the absence of chloride entirely as the lanthanide series is traversed. However, it is less direct for the actinides. A typical change in ionic radius for adjacent actinides in the same oxidation state with the same coordination number is approximately 0.01 Å.[60] As the actinide contraction is larger than one would expect between plutonium and americium, it is not entirely surprising that americium would elect to exclude chloride from the inner coordination sphere. Furthermore, it does not explain the renewal of the chloride moiety in the curium structure where the curium is smaller and slightly "harder" than americium. It appears that the notion of ionic and steric factors as the largest contributors to the products of the f-block elements is not entirely true for the actinides, and other factors such as an increased involvement of the 5*f*/6*d* orbitals, as well as the metal itself must be considered.

Electronic Structure Calculations (Collaboration with Laura Gagliardi's Group). Insights into the bonding of the 5*f* and 4*f* orbitals were obtained through electronic structure analyses of **PuBOCl-1**, **PuBOCl-2**, **AmBO**, **CmBO**, **CmBOCl**, and **CeBOCl** at the CASSCF level, respectively. Selected molecular orbitals in the HOMO-LUMO region involving the 5*f* and 4*f* orbitals are depicted in Figures 10 and 11.

Considering the actinide borates, the active space for **PuBOCl-1** and **PuBOCl-2**, **AmBO**, and **CmBO** and **CmBOCl** included five, six, and seven electrons in seven 5*f* orbitals and an additional doubly occupied orbital, respectively. In regards to the relative state energies, for **PuBOCl-1** and **PuBOCl-2**, the quartet states were predicted to be an average 45 kcal/mol higher in energy than the sextet state at the CASPT2 level, respectively, while for **AmBO**, the quintet state was 47 kcal/mol higher in energy than the septet state at the same level. With an electronic structure of Cm $5f^7$, the half-filled *f*-orbitals affords significant stability for **CmBO** and **CmBOCl**, and consistently, the sextet states are

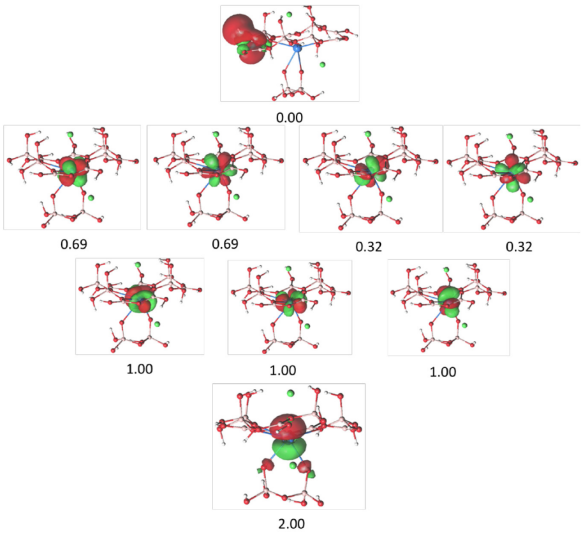

Figure 10. Molecular orbitals responsible for the bonding in **PuBOCl-1** (sextet) at the CASSCF level. Respective occupation numbers are indicated below the orbital plots (isovalue 0.04). Pu, blue; Cl, bright green; O, red; B, light pink; and H, white.

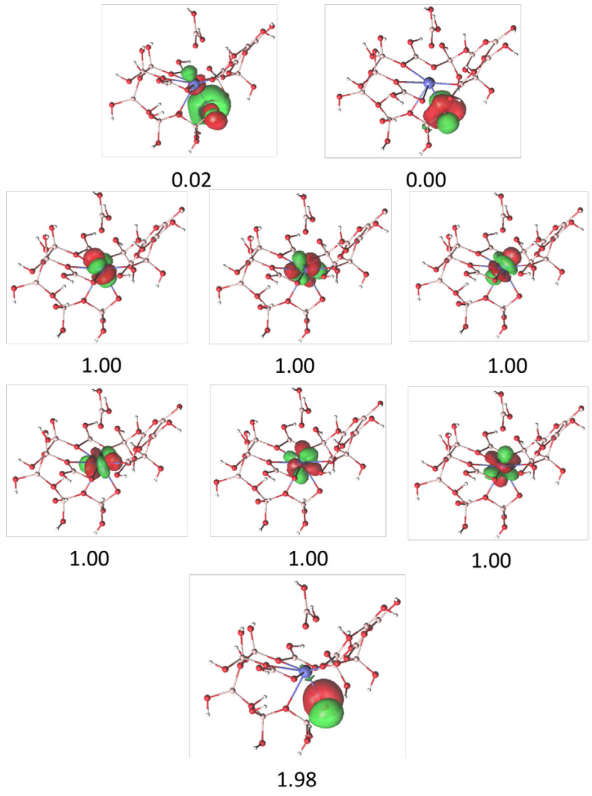

Figure 11. Molecular orbitals responsible for the bonding in **AmBO-1** (septet) at the CASSCF level. Respective occupation numbers are indicated below the orbital plots (isovalue 0.04). Am, blue; O, red; B, light pink; and H, white.

predicted to be an average 97 kcal/mol above the ground octet state, respectively.

Irrespective of structure and actinide metal, the 5*f* orbitals are all localized on the metal site. There is no evident interaction of the An 5*f* orbitals with the immediate coordinating atoms. However, a unique orbital picture is depicted just below the valence 5*f* orbitals. For **PuBOCl-1**, there is a Pu 6*p* orbital, which shows delocalization to an O 2*p* orbital of the basal B_2O_7 ligand (Figure 10). For **AmBO**, immediately below the valence Am 5*f* orbitals, there is a doubly occupied O 2*p* orbital on the basal BO_4 tetrahedra showing delocalization toward an Am 6*d* orbital (Figure 11). Unlike the Pu structures, the Am 6*p* orbital lies much lower in energy than the Am 5*f*. As observed in **AmBO**, an O 2*p* orbital on the basal BO_4 ligand illustrates delocalization toward a Cm 6*d* orbital in **CmBO**.

Consistent with the doublet ground state for **CeBOCl**, a single Ce 4*f* orbital is localized on the metal site with no apparent interaction with any atomic orbitals of the coordinating ligands. This orbital picture is similar to what is observed for the An^{3+} borates where the An 5*f* orbitals were all localized on the metal. Just below this Ce 4*f* SOMO, there is a localized Ce 5*p* orbital as analogously observed in **PuBOCl-1**. However, there is no apparent interaction of the Ce 5*p* orbital with any of the basal coordinating atoms.

Additional electronic structure analyses were performed at the PBE/def-TZVP level. For **PuBOCl-1**, **PuBOCl-2**, and **AmBO**, the five and six highest SOMOs are localized An 5*f* orbitals. However, just below the localized valence An 5*f* orbitals are additional An 5*f* orbitals, which show bonding with the O 2*p* orbitals of the basal borate ligands. However, for **CmBO** and **CmBOCl**, the orbital picture is slightly different in that the seven highest SOMOs are localized Cm 5*f* orbitals with no observed interaction with coordinating atoms. For **CeBOCl**, the highest SOMO corresponds to a localized Ce 4*f* orbital, and there are four orbitals that illustrate bonding between Ce 4*f* and O 2*p* orbitals of the coordinating basal borate ligands, as analogously observed in **PuBOCl-1**, **PuBOCl-2**, and **AmBO**.

REFERENCES CITED

1. T. Nakano and E. Nakamura, *Phys. Earth Planet. Inter.*, 2001, **127**, 233-252.
2. S. R. Taylor, *Geochim. Cosmochim. Acta*, 1964, **28**, 1273-1285.
3. P. C. Burns, R. C. Ewing and F. C. Hawthorne, *Can. Mineral.*, 1997, **35**, 1551-1570.
4. P. C. Burns, *Can. Mineral.*, 2005, **43**, 1839-1894.
5. P. C. Burns, M. L. Miller and R. C. Ewing, *Can. Mineral.*, 1996, **34**, 845-880.
6. (a) I. A. Donald, B. L. Metcalfe and R. N. J. Taylor, *J. Mater. Sci.*, 1997, **32**, 5851-5887; (b) W. E. Lee, M. I. Ojovan, M. C. Stennett and N. C. Hyatt, *Adv. Appl. Ceram.*, 2006, **105**, 3-12.
7. B. Grambow, *elements*, 2006, **2**, 357-364.
8. W. Lutze, *Glass*, in *Uncertainty Underground*, ed. A. M. Macfarlane and R. C. Ewing, The MIT Press, London, 2006, chapter 21, pp. 353–364.
9. A. C. Snider, *Verification of the Definition of Generic Weep Brine and the Development of a Recipe for This Brine*. ERMS 527505. Carlsbad, NM: Sandia National Laboratories, 2003.
10. M. Borkowski, M. Richmann, D. T. Reed and Y. Xiong, *Radiochim. Acta*, 2010, **98**, 577-582.
11. H. Behm, *Acta Cryst.*, 1985, **C41**, 642-645.
12. M. Gasperin, *Acta Cryst.*, 1987, **C43**, 1247-1250.
13. M. Gasperin, *Acta Cryst.*, 1987, **C43**, 2031-2033.

14. M. Gasperin, *Acta Cryst.*, 1987, **C43**, 2264-2266.
15. M. Gasperin, *Acta Cryst.*, 1988, **C44**, 415-416.
16. M. Gasperin, *Acta Cryst.*, 1989, **C45**, 981-983.
17. M. Gasperin, *Acta Cryst.*, 1990, **C46**, 372-374.
18. A. Cousson and M. Gasperin, *Acta Cryst.*, 1991, **C47**, 10-12.
19. D. L. Clark, D. E. Hobart and M. P. Neu, *Chem. Rev.*, 1995, **95**, 25-48.
20. S. Wang, E. V. Alekseev, J. Ling, G. Liu, W. Depmeier and T. E. Albrecht-Schmitt, *Chem. Mater.*, 2010, **22**, 2155-2163.
21. S. Wang, E. V. Alekseev, J. T. Stritzinger, W. Depmeier and T. E. Albrecht-Schmitt, *Inorg. Chem.*, 2010, **49**, 2948-2953.
22. S. Wang, E. V. Alekseev, J. T. Stritzinger, W. Depmeier and T. E. Albrecht-Schmitt, *Inorg. Chem.*, 2010, **49**, 6690-6696.
23. S. Wang, E. V. Alekseev, J. T. Stritzinger, G. Liu, W. Depmeier and T. E. Albrecht-Schmitt, *Chem. Mater.*, 2010, **22**, 5983-5991.
24. S. Wang, E. V. Alekseev, J. Ling, S. Skanthakumar, L. Soderholm, W. Depmeier and T. E. Albrecht-Schmitt, *Angew. Chem. Int. Ed.*, 2010, **49**, 1263-1266.
25. S. Wang, E. V. Alekseev, J. Diwu, H. M. Miller, A. Oliver, G. Liu, W. Depmeier and T. E. Albrecht-Schmitt, *Chem. Mater.*, 2011, **23**, 2931-2939.
26. S. Wang, E. V. Alekseev, H. M. Miller, W. Depmeier and T. E. Albrecht-Schmitt, *Inorg. Chem.*, 2010, **49**, 9755-9757.
27. J. P. Kaszuba and W. H. Runde, *Environ. Sci. Technol.*, 1999, **33**, 4427-4433.
28. Z. Yoshida, S. G. Johnson, T. Kimura and J. R. Krsul, *Neptunium*, in *The Chemistry of the Actinide and Transactinide Elements*, ed. L. R. Morss, N. M. Edelstein and J. Fuger, Springer, The Netherlands, 2006, vol. 2, chapter 6, pp. 753-770.
29. T. H. Bray, J. Ling, E. S. Choi, J. S. Brooks, J. V. Beitz, R. E. Sykora, R. G. Haire, D. M. Stanbury and T. E. Albrecht-Schmitt, *Inorg. Chem.*, 2007, **46**, 3663-3668.
30. L. Rao, *Chem. Soc. Rev.*, 2007, **36**, 881-892.
31. M. Buhl, G. Schreckenbach, N. Sieffert and G. Wipff, *Inorg. Chem.*, 2009, **48**, 9977-9979.
32. A. K. Pikaev, A. V. Gogolev and V. P. Shilov, *Radiat. Phys. Chem.*, 1999, **56**, 483-491.
33. P. Almond, R. Sykora, S. Skanthakumar, L. Soderholm and T. Albrecht-Schmitt, *Inorg. Chem.*, 2004, **43**, 958-963.
34. I. Charushnikova, E. Boss, D. Guillaumont and P. Moisy, *Inorg. Chem.*, 2010, **49**, 2077-2082.
35. S. Cornet, L. Häller, M. Sarsfield, D. Collison, M. Helliwell, I. May and N. Kaltsoyannis, *Chem. Commun.*, 2009, 917-919.
36. M. Grigor'ev, A. Fedoseev and N. Budantseva, *Russ. J. Coord. Chem.*, 2003, **29**, 877-879.
37. P. C. Burns, K.-A. Kubatko, G. Sigmon, B. J. Fryer, J. E. Gagnon, M. R. Antonio and L. Soderholm, *Angew. Chem. Int. ed.*, 2005, **44**, 2135-2139.
38. P. C. Burns, J. D. Grice and F. C. Hawthorne, *Can. Mineral.*, 1995, **33**, 1131-1151.
39. J. D. Grice, P. C. Burns and F. C. Hawthorne, *Can. Mineral.*, 1999, **37**, 731-762.
40. G. Yuan and D. Xue, *Acta. Cryst.*, 2007, **B63**, 353-362.
41. E. L. Belokoneva, *Cryst. Res. Technol.*, 2008, **43**, 1173-1182.
42. M. Touboul, N. Penin and G. Nowogrocki, *Solid State Sci.*, 2003, **5**, 1327-1342.
43. C. Dendrinou-Samara, C. M. Zaleski, A. Evagorou, J. W. Kampf, V. L. Pecoraro and D. P. Kessissoglou, *Chem. Commun.*, 2003, **21**, 2668-2669.

44. T. Okubo, H. Kuwamoto, K. H. Kim, S. Hayami, A. Yamano, M. Shiro, M. Maekawa and T. Kuroda-Sowa, *Inorg. Chem.*, 2011, **50**, 2708-2710.
45. J. C. Sullivan, J. C. Hindman and A. J. Zielen, *J. Am. Chem. Soc.*, 1961, **83**, 3373-3378.
46. N. N. Krot and M. S. Grigor'ev, *Russ. Chem. Rev.*, 2004, **73**, 89-100.
47. H. A. Friedman and L. M. Toth, *J. Inorg. Nucl. Chem.*, 1980, **42**, 1347 – 1349.
48. N. M. Edelstein, *Magnetic Properties*, in *The Chemistry of the Actinide and Transactinide Elements*, ed. L. R. Morss, N. M. Edelstein and J. Fuger, Springer, The Netherlands, 2006, vol. 4, chapter 20, pp. 2225-2306.
49. T. Nakamoto, M. Nakada and A. Nakamura, *Solid State Commun.*, 2001, **119**, 523-526.
50. T. Z. Forbes, P. C. Burns, S. Skanthakumar and L. Soderholm, *J. Am. Chem. Soc.*, 2007, **10**, 2760-2761.
51. S. Wang, E. V. Alekseev, W. Depmeier and T. E. Albrecht-Schmitt, *Chem. Com.*, 2010, **46**, 3955-3957.
52. S. Wang, E. M. Villa, J. Diwu, E. V. Alekseev, W. Depmeier and T. E. Albrecht-Schmitt, *Inorg. Chem.*, 2011, **50**, 2527-2533.
53. C. Apostolidis, B. Schimmelpfennig, N. Magnani, P. Lindqvist-Reis, O. Walter, R. Sykora, A. Morgenstern, E. Colineau, R. Caciuffo, R. Klenze, R. G. Haire, J. Rebizant, F. Bruchertseifer and T. Fanghanel, *Angew. Chem. Int. Ed.*, 2010, **49**, 6343-6347.
54. G. Liu and J. V. Beitz, *Spectra and Electronic Structures of Free Actinide Atoms*, in *The Chemistry of the Actinide and Transactinide Elements*, ed. L. R. Morss, N. M. Edelstein and J. Fuger, Springer, The Netherlands, 2006, vol. 4, chapter 16, pp. 2013-2111.
55. A. C. Bean, B. L. Scott, T. E. Albrecht-Schmitt and W. Runde, *Inorg. Chem.*, 2003, **42**, 5632-5636.
56. T. Z. Forbes and P. C. Burns, *Can. Mineral.*, 2007, **45**, 471-477.
57. D. L. Clark, S. S. Hecker, G. D. Jarvinen and M. P. Neu, *Plutonium*, in *The Chemistry of the Actinide and Transactinide Elements*, ed. L. R. Morss, N. M. Edelstein and J. Fuger, Springer, The Netherlands, 2006, vol. 2, chapter7, pp. 813-1264.
58. S. Wang, E. V. Alekseev, W. Depmeier and T. E. Albrecht-Schmitt, *Inorg. Chem.*, 2011, **50**, 2079-2081.
59. Edelstein, N. M.; Fuger, J.; Katz, J. J.; Morss, L. R. *The Chemistry of the Actinide and Transactinide Elements* (Eds.: L. R. Morss, N. M. Edelstein, J. Fuger), Springer, The Netherlands, **2006**.

60. Shannon, R. D. *Acta Crystallogr. Sect. A* **1976**, 32, 751-767.
61. (a) Skanthakumar, S.; Antonio, M.R., Wilson, R.E.; Soderholm, L. *Inorg. Chem*. **2007**, 46, 3485-3491. (b) Apostolidis, C.; Schimmelpfennig, B.; Magnani, N.; Lindqvist-Reis, P.; Walter, O.; Sykora, R.; Morgenstern, A.; Colineau, E.; Caciuffo, R.; Klenze, R.; Haire, R. G.; Rebizant, J.; Bruchertseifer, F.; Fanghanel, T. *Angew. Chem. Int. Ed.* **2010**, *49*, 6343. (c) Matonic, J. H.; Scott, B. L.; Neu, M.P. *Inorg. Chem*. **2001**, 40, 2638-2639.
62. (a) Nash, K. L.; Lavallette, C.; Borkowski, M.; Paine, R. T.; Gan, X. *Inorg. Chem*. **2002**, 41, 5849-5858. (b) Miguirditchian, M.; Guillaneux, D.; Guillaumont, D.; Moisy, P.; Madic, C.; Jensen, M. P.; Nash, K. L. *Inorg. Chem*. **2005**, 44, 1404-1412.
63. (a) Lu, P.; Wang, Y.; Lin, J.; You, L. *Chem. Comm.*, **2001**, 1178-1179. (b) Li, L.; Lu, P.; Wang, Y.; Jin, X.; Li, G.; Wang, Y.; You, L.; Lin, J. *Chem. Mater*. **2002**, 14, 4963-4968. (c)Li, L.; Jin, X.; Li, G.; Wang, Y.; Liao, F.; Yao, G.; Lin, J. *Chem. Mater*. **2003**, 15, 2253-2260.

64. Cong, R.; Yang, T.; Wang, Z.; Sun, J.; Liao, F.; Wang, Y.; Lin, J. *Inorg. Chem*. **2011**, 50, 1767-1774.

65. Belokoneva, E.L.; Stefanovich, S.; Dimitrova, O.V.; Ivanova, A.G. *Zh. Neorg. Khim.* **2002,** 47, 370-377.

66. Ruiz-Martínez, A.; Alvarez, S. *Chem. Eur. J*. **2009**, 15, 1470-7480.

67. Ruiz-Martínez, A.; Casanova, D.; Alvarez, S. *Chem. Eur. J*. **2008**, 14, 1291-1303.

68. Polinski, M. J.; Wang, S.; Alekseev, E. V.; Depmeier, W.; Albrecht-Schmitt, T. E. *Angew. Chem. Int. Ed.* **2011**, 50, 8891-8894.

69. Polinski, M. J.; Wang, S.; Alekseev, E. V.; Depmeier, W.; Liu, G.; Haire, R. G.; Albrecht-Schmitt, T. E. *Angew. Chem. Int. Ed.* **2012**, 51, 1869-1872.

70. Borgoo, A.; Torrent-Sucarrat, M.; De Proft, F.; Geerlings, P. *J. Chem. Phys*. **2007**, 126, 234104.

71. Goodey, J.; Broussard, J.; Halasyamani, P. S. *Chem. Mater.*, **2002**, *14*, 3174-3180.

72. Sykora, R. E.; Assefa, Z.; Haire, R. G.; Albrecht-Schmitt, T. E. *Inorg. Chem.* **2005**, 44, 5567-5676.

73. Sykora, R. E.; Assefa, Z.; Haire, R. G.; Albrecht-Schmitt, T. E. *Inorg. Chem.* **2006**, 45, 475-477.

74. J. E. Birkett, M. J. Carrott, O. D. Fox, C. J. Jones, C. J. Maher, C. V. Roube, R. J. Taylor, D. A. Woodhead, *Chimia* **2005**, *59*, 898-904.

75. a) R. D. Shannon, *Acta Cryst.* **1976**, *A32*, 751-767; b) K. L. Nash, *Solvent Extr. Ion Exch.* **1993**, *11*, 729-728. c) C. Apostolidis, B. Schimmelpfennig, N. Magnani, P. Lindqvist-Reis, O. Walter, R. Sykora, A. Morgenstern, E. Colineau, R. Caciuffo, R. Klenze, R. G. Haire, J. Rebizant, F. Bruchertseifer, T. Fanghanel, *Angew. Chem. Int. Ed.* **2010**, *49*, 6343-6347.

76. B. Weaver, F. A. Kappelmann, *ORNL Report*, 1964.
77. D. Warin, in 'Actinide and Fission Product Partioning and Transmutation, 7th Information Exchange Meeting, Jeju, Republic of Korea, 14–16 October, 2002', Nuclear Energy Agency, OECD, Paris, **2003**, p.53.
78. Jensen, M. P.; Bond, A. H. *J. Am. Chem. Soc.* **2002**, *124*, 9870-9877.
79. W. H. Runde, B. L. Mincher, *Chem. Rev.* **2011**, *111*, 5723-5741.
80. J. M. Adnet, L. Donnet, P. Brossard, J. Bourges, U.S. patent 5609745 (March 11, 1997).
81. B. J. Mincher, L. R. Martin, N. C. Schmitt, *Inorg. Chem.* **2008**, *47*, 6984-6989.
82. C. Madic, in 'Actinide and Fission Product Partioning and Transmutation, Sixth Information Exchange Meeting, Madrid, Spain, 11–13 December 2000', Nuclear Energy Agency, OECD, Paris, **2001**, p.53.
83. C. Ye, J. M. Shreeve, *J. Org. Chem.* **2004**, *69*, 6511-6513.
84. Solomon, E. I.; Hedman, B.; Hodgson, K. O.; Dey, A.; Szilagyi, R. K. *Coord. Chem. Rev.* **2005***, 249*, 97.

85. Kozimor, S. A.; Yang, P.; Batista, E. R.; Boland, K. S.; Burns, C. J.; Clark, D. L.; Conradson, S. D.; Martin, R. L.; Wilkerson, M. P.; Wolfsberg, L. E. *J. Am. Chem. Soc*. **2009**, 131(34), 12125.

86. Minasian, S. G.; Keith, J. M.; Batista, E. R.; Boland, K. S.; Christensen, C. N.; Clark, D. L.; Conradson, S. D.; Kozimor, S. A.; Martin, R. L.; Schwarz, D. E.; Shuh, D. K.; Wagner, G. L.; Wilkerson, M. P.; Wolfsberg, L. E.; Yang, P. *J. Am. Chem. Soc.* **2012**, *134*, 5586-5597.
87. Hoch, C. Zeitschrift fuer Naturforschung, B **2011**, *66*, 1248.
88. Keszler, D. A.; Sun, H. Acta Crystallographica C **1988**, *44*, 1505.

89. Huber, M.; Deiseroth, H. J. Zeitschrift fuer Kristallographie **1995**, *210*, 685.